Proceedings of the ASME 2010 3rd Joint US-European Fluids Engineering Summer Meeting and 8th International Conference on Nanochannels, Microchannels, and Minichannels
FEDSM-ICNMM2010
August 1-5, 2010, Montreal, Canada

FEDSM-ICNMM2010-30227

THE EFFECT OF FLOW PULSATIONS ON THE STREAMWISE VIBRATION OF A CANTILEVERED RIGID CYLINDER

Efstathios Konstantinidis
Dimitris Giagopoulos
Department of Mechanical Engineering
University of Western Macedonia, Kozani 50100, Greece
Email: {ekonstantinidis, dgiagopoulos}@uowm.gr

Joseph Sherwood
Stavroula Balabani
Department of Mechanical Engineering
King's College London, Strand WC2R 2LS, U.K.
Email: {joseph.sherwood, stavroula.balabani}@kcl.ac.uk

ABSTRACT

The effect of pulsations superimposed on a mean incident flow on the streamwise vibration of an elastically-supported cantilevered rigid cylinder with two coupled translational and rotational degrees of freedom was investigated experimentally. The pulsation frequency was varied between 7.8 – 19.2 Hz corresponding to 1.2 – 3.0 times the vortex shedding frequency from a fixed cylinder in steady flow whereas the amplitude of the pulsations and the incident-flow mean velocity were held constant, the latter corresponding to a Reynolds number of 2160. The results show that there are two excitation regions in which the amplitude of vibration increases up to 400% compared to that in steady flow at the same Reynolds number. As the pulsation frequency is further increased in each range, the amplitude of the vibrations drops almost linearly down to a level near that without flow pulsations although the frequency of vibration remains locked-on at the imposed pulsation frequency in all cases.

NOMENCLATURE

$A_{\rm rms}$	Root-mean-square of cylinder's tip displacement
C_a	Added mass coefficient
D	Cylinder diameter
f_c	Frequency of cylinder vibration
f_e	Pulsation (excitation) frequency
f_0	Frequency of vortex shedding from a fixed cylinder
f_w	Frequency of wake fluctuations
L_e	Effective length of the cylinder
m^*	Mass ratio
Re	Reynolds number
t	Time
u	Instantaneous flow velocity
U	Phase-averaged flow velocity
U_0	Incident-flow mean velocity
ΔU	Amplitude of velocity pulsation

Greek letters

ζ	Damping factor
θ	Angular deflection of the cylinder
ξ	Tip displacement
ϕ	Phase-angle of the pulsation waveform
ϕ_s	Phase-angle shift of the pulsation waveform

INTRODUCTION

The interaction of steady and unsteady incident flows and vibrating compliant structures poses a fundamental problem which has important practical implications in engineering applications. A variety of structures exposed to external flows such as heat-exchangers tubes, offshore platforms and risers, power-transmition lines, stacks, chimneys, bridges, etc., are susceptible to flow-induced vibration which can lead to fatigue damage or even failure. The real problems are too complicated to analyze meaningfully, therefore design guidelines are often based on empirical data from simplified flow configurations. Vibrations of cylindrical structures may be excited by turbulence, vortex shedding and/or incident waves. Among these excitation mechanisms, the study of the so-called 'vortex-induced vibrations' has received much attention over the years and still continues to attract considerable interest, probably due to its complexity. Most of the previous work has concentrated on single degree-of-freedom systems of elastically-mounted circular cylinders vibrating in the streamwise or transverse directions with respect to steady uniform incident flows. Pertinent reviews on this type of flow-induced vibrations can be found in Refs [1–3].

Streamwise vibrations of flexibly-supported circular cylinders with a single translational degree-of-freedom have, since long, been associated with alternating and symmetric vortex shedding giving rise to two separate excitation branches in the amplitude response [2, 4]. A failure of a thermocouple well in Japan's Monju fast breeder reactor in 1995 stipulated some interest in the study of the streamwise response of flexibly-supported and cantilevered cylinders and valuable insight on the vibration response and the wake patterns was obtained for low values of the mass–damping parameter [5]. The results were in agreement with early findings and confirmed the existence of two positive excitation branches. A more recent study, also from Japan, on the effect of forced streamwise oscillations on the forces and wake patterns also identified two regions of negative damping (positive excitation in free vibrations) [6]. For the simplified two-dimensional configuration, the response amplitude of the cylinder remains constant along the span. However, for engineering structures such as long flexible risers or cables, vibrations can exhibit significant spanwise amplitude variation which might affect the dynamics of the flow/structure interaction. For example, it has been demonstrated that a cantilevered cylinder exhibits a single unified streamwise vibration branch with excitation attributed mostly to symmetric shedding [5]. This type of vibration might be approximated by a 'single' rotational degree-of-freedom of a cantilevered rigid cylinder. More complex vibrations involving combinations of different degrees of freedom, such as coupled translational and rotational vibrations, have not been considered so far.

Flow pulsations may act as an extraneous excitation source of flow-induced vibrations. The alternating and symmetric vortex shedding modes observed in the wake of cylinders vibrating freely in the streamwise direction can also be excited by the superimposition of streamwise pulsations on a non-zero mean incident flow over fixed cylinders [7, 8]. In fact, this type of excitation is kinematically equivalent to the streamwise oscillation of a cylinder in a steady flow if the pulsation wavelength is long compared to the diameter of the cylinder [9]. This analogy has resulted in a paradoxical phenomenon; the response of a streamwise vibrating cylinder is negligible for conditions at which the fluid forcing on the cylinder is expected to be magnified by vortex shedding lock-on [7]. Hence, self-excited vortex-induced vibrations are not like a classical resonance phenomenon where both the forcing and the response are mutually amplified.

The scope of the present work is to investigate the effect of flow pulsations on the streamwise vibration of an elastically-supported cantilevered cylinder. This configuration involves a competition of intrinsic and extraneous fluid-excitation mechanisms and may lead to a new rationale for understanding the nature of the complex flow/structure interactions.

MATERIALS AND METHODS

Flow Configuration and Test Cylinder

The flow configuration employed in the experiments is a closed-loop water tunnel with a 72 mm × 72 mm working area. The facility was designed to deliver both steady and pulsating flows past a fixed cylinder as described in a number of previous publications [8, 10–12]. The velocity profile of the incident flow was found to be uniform within ±0.5%, excluding the boundary layers on the walls, and the turbulence intensity was approximately 3% for bulk-flow velocities up to 1.0 m/s.

A rigid cylinder made of Perspex and 7.2 mm in diameter was supported at one end on a steel-plate spring positioned inside an external cavity attached to the side of the working area as shown in Fig. 1. The other end of the cylinder was free and protruded into the working area at a small clearance from the wall. As the main portion of the cylinder was subjected to water flow, hydro-elastic vibrations were excited. The aspect ratio of the effective length of the cylinder immersed in fluid flow to the cylinder diameter was $L_e/D \approx 10$. Figure 2 shows the details of the cylinder/plate-spring assembly. The test cylinder was made hollow in order to reduce its mass as much as possible. The mass ratio of the cylinder to that of the displaced fluid was estimated at $m^* = 1.21$. The plate spring was securely clamped on both ends to the retaining blocks which are fixed to the walls of the external cavity. With this arrangement the vibration of the cylinder was restricted in the flow (streamwise) direction only, involving a coupled translational and rotational motion as a result of normal bending and torsion of the plate spring, respectively.

Flow pulsations of adjustable amplitude and frequency can be superimposed on a steady component via a rotating valve driven by a variable speed motor. Figure 3 shows an example of the instantaneous velocity for pulsed incident flow. The incident-flow pulsation contains some high-frequency fluctuations on top of the main component due to background turbulence. For the flow conditions employed, the pulsation waveform can be approximated by a sinusoidal function of the phase-angle,

$$U(\phi) = U_0 + \Delta U \sin(2\pi f_e t + \phi_s) \quad (1)$$

where U_0 is the incident-flow mean velocity and ΔU is the amplitude of the pulsations. The phase-angle relates to time via $\phi = 2\pi f_e t$ with f_e being the excitation frequency of the controlled pulsations. The phase-angle was measured with an

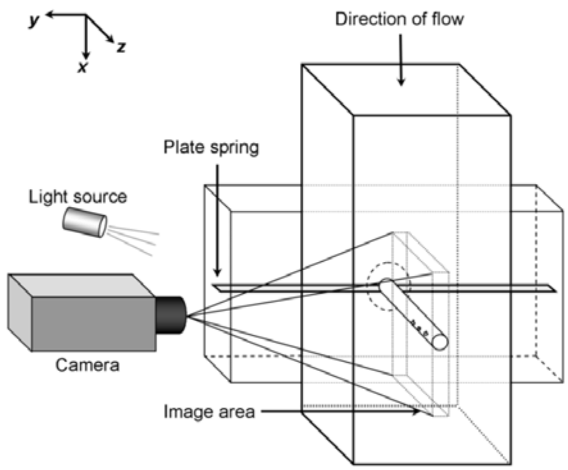

FIGURE 1. SCHEMATIC OF THE EXPERIMENTAL SETUP.

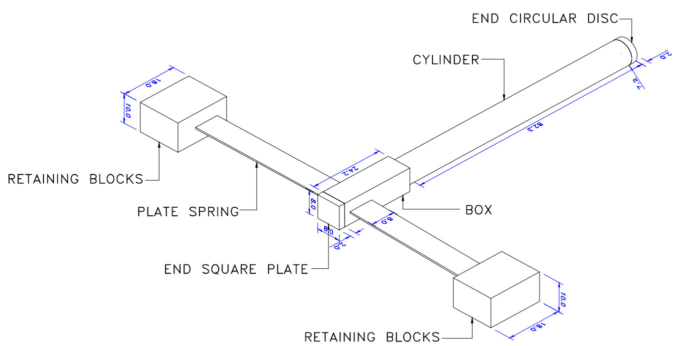

FIGURE 2. ASSEMBLY OF THE SPRING/CYLINDER [13].

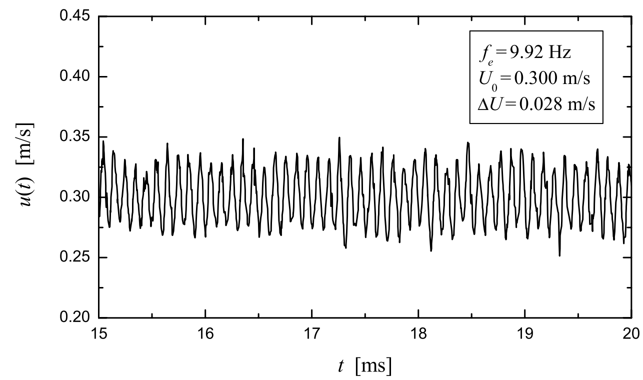

FIGURE 3. EXAMPLE OF THE INCIDENT-FLOW VELOCITY.

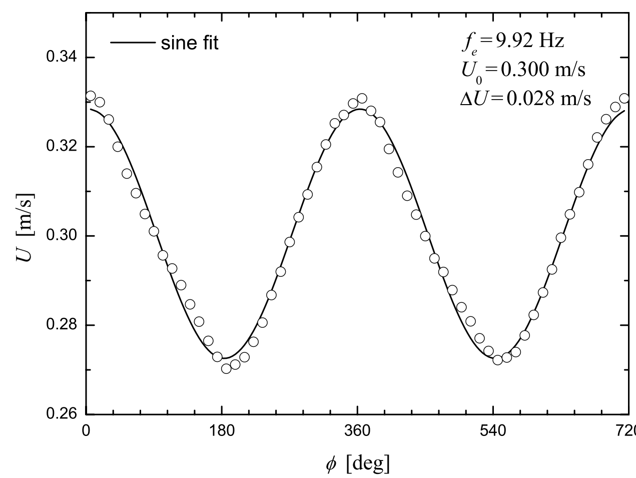

FIGURE 4. PHASE-AVERAGED MEAN VELOCITY WAVEFORM OF THE INCIDENT PULSED FLOW.

optical encoder (2000 pulses per revolution plus a reference pulse) attached to the shaft of the rotating valve. A phase-shift is implemented in Eq. (1) since the phase-angle varies with the pulsation frequency. Figure 4 illustrates the goodness of the sine fit to the phase-averaged velocity waveform of the data shown in Fig 3.

Measurement Techniques

An imaging technique was implemented in order to track the motion of the vibrating cylinder. A high-speed digital camera was used to capture instantaneous images of two reflecting features attached to the side of the cylinder and close to its free end which were illuminated by an external light source as shown in Fig. 1. Appropriate image-processing algorithms were employed in order to determine the centroid of each reflecting feature. This methodology resulted in both the instantaneous tip displacement $\xi(t)$ of the cylinder and its angular deflection $\theta(t)$. The displacement signal was further processed using the fast Fourier transform in order to compute the power-spectral density and determine the dominant vibration frequencies.

A single-component laser-Doppler system was employed to measure the velocity fluctuations of the incident flow upstream of the cylinder and in its wake. The latter measurements were obtained at a station approximately 3.2D downstream of the cylinder's rest location and half-way along the cylinder span. For the results reported here the measuring probe was placed between 0.5-1.0D off the wake centerline where the streamwise velocity fluctuations were strongest in order to determine the vortex shedding frequencies and supplement the vibration measurements. In addition, the flow rate was measured by an electromagnetic flow-meter.

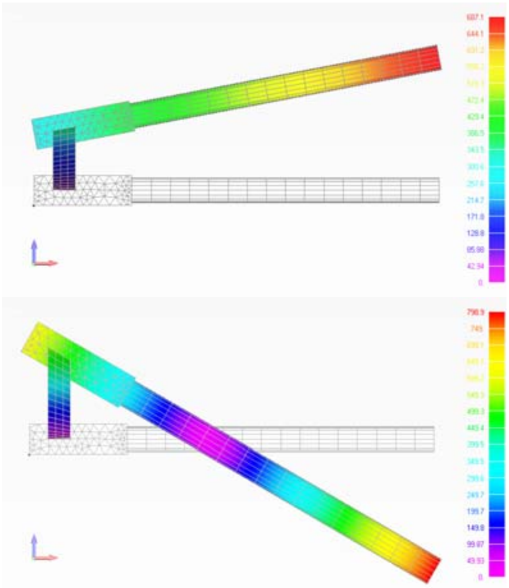

FIGURE 5. FIRST AND SECOND MAIN VIBRATION MODES OF THE CYLINDER/PLATE-SPRING SYSTEM.

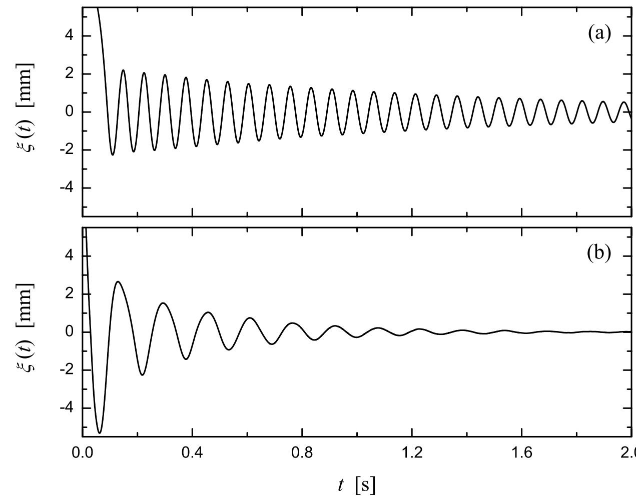

FIGURE 6. FREE DECAY TESTS IN AIR (a) AND WATER (b).

Vibration Modes

The mode shapes and the natural frequencies of the cylinder-spring plate assembly were determined ad hoc by finite-element analysis through appropriate software (ANSA, DYNAMIS). The structural model was geometrically discretized by solid (tetrahedral) and shell (quadrilateral) elements having 4034 degrees of freedom. The analysis indicated that there are two main vibration modes both involving coupled rotational and translational motion of the cylinder with natural frequencies of 13.2 and 32.0 Hz (in vacuum). Other vibration modes are not considered either because their natural frequencies were either much higher than the frequencies of interest here (i.e. $>$ 100 Hz) or could not be excited, e.g. the rotation of the cylinder around its axis. Figure 5 shows the two main vibration mode shapes. The basic difference between them is that the rotational and translational components of the tip displacement are in the same direction (in-phase) in the first mode whereas they point in opposite directions (out-of-phase) in the second mode.

Free decay tests were carried out in quiescent air and water. The impulse response to tapping the free end of the cylinder was measured and some representative tests are shown in Fig. 6. As seen, essentially only one dominant vibration mode is evident by visual observation in both fluid media. Initially, an exponential decay single-frequency sinusoid was fitted to the data by the method of least squares in order to determine the natural frequency and damping of the dominant mode [14]. The curve fit for the data in still air resulted in a natural frequency of 13.1 Hz and a damping ratio of 0.009. The measured natural frequency in still air is very close to that determined by the finite-element analysis (in vacuum). However, the natural frequency decreased to 6.4 Hz and the damping factor increased to 0.06 in still water due to added mass and added damping effects. A rough estimate of the ratio of the natural frequency in still water to that in vacuum (or still air) may be obtained by $\sqrt{m^*/(m^*+C_a)}$ where C_a is the added mass coefficient for a circular cylinder ($C_a = 1.0$). This expression results in a ratio of 0.74 which is higher than the ratio of 0.49 obtained from the measurements. This difference might be attributed to the fact that the plate-spring was also immersed in still water (inside the external cavity) and there are added-mass and added damping effects associated with its vibration.

An auto-regressive moving average (ARMA) model was employed in order to deduce the natural frequencies and damping of the fluid-structure system. ARMA is a system identification method which can be used to represent the time series of inputs–outputs as a linear combination of past values plus white noise to a specified order. This method has been previously used to determine fluid damping of an elastic cylinder in cross-flow [15]. The same approach is employed here for the time series of the displacements from tapping tests in still fluid. It should be pointed out that the structure and the fluid are considered as a single combined dynamical system. The ARMA model can be used to identify the parameters of the different vibration modes with uncertainties of $\pm 10\%$. However, the results are sensitive to the selection of the model order. For the present analysis an order of 10 for data and 3 for noise were selected and it was verified that this is the optimal choice by the Akaike criterion [16]. Table 1 lists the fluid-structure parameters estimated by the ARMA model (the combined mass–damping $m^*\zeta$ parameter is also shown for reference). The predicted natural frequencies f_n and the damping ratios ζ of the first mode are very similar to

TABLE 1. NATURAL FREQUENCIES AND DAMPING FACTORS ESTIMATED FROM FREE DECAY TESTS IN STILL FLUID USING AN ARMA MODEL

	Air		Water	
f_n (Hz)	13.1	26.3	6.4	13.4
ζ	0.009	0.010	0.067	0.081
$m^*\zeta$	0.011	0.012	0.081	0.098

those obtained by curve-fitting which gives some credence to the model results. The main advantage of the ARMA model is that it also provides an estimate for the parameters of the second mode which could not be obtained otherwise. The natural frequency of the second mode in still air (26.3 Hz) predicted by the ARMA model is very close to the harmonic of the first-mode natural frequency and differs from that predicted by the finite-element analysis. This difference is not unexpected since both modeling approaches are subject to non-trivial approximations. In still water, the ARMA model shows that natural frequencies reduce approximately by half whereas damping ratios increase by a factor of eight. The values obtained in still water are consistent with the results reported for water cross-flow in the following sections.

RESULTS AND DISCUSSION

Steady Flow

A summary of the response of the vibrating cylinder for steady incident flow is provided prior to the presentation of the pulsed-flow results for reference. Measurements were obtained for flow velocities in the range $U_0 = 0.02 - 0.40$ m/s corresponding to Reynolds numbers $Re = 130 - 2840$. Within this range of Reynolds numbers the flow regime changes from laminar wake to transition to turbulence in the shear layers on the basis of results for stationary cylinders [17]. Most of the measurements correspond to the latter regime and any effects due to the Reynolds number might be limited to the first couple of flow velocities examined. Figure 7 shows the r.m.s. amplitude A_{rms} and the dominant frequencies of the cylinder vibrations f_c as a function of the flow velocity. The measured wake frequency f_w is also shown on the right axis of the lower plot whereas a straight line indicates the vortex shedding frequency anticipated in the wake of a fixed cylinder, f_0. The response can be divided into two separate ranges of flow velocities. The first range ($U_0 <$ 0.14 m/s) corresponds to the excitation of the first eigenmode of the structure at a single predominant frequency. Within the first range, the amplitude-response rises to 5.3% of the cylinder diameter (note the dimensionless values on the right axis of the upper plot). For flow velocities $U_0 > 0.14$ m/s, the vibration of the cylinder involves a coupled excitation of both structural eigenmodes associated with two separate natural frequencies. The amplitude initially drops off in the second range (or response branch), then increases up to 5.0% of the cylinder diameter, followed by a gradual drop at the highest flow velocities. It can also be seen that the frequency of the velocity fluctuations in the wake of the vibrating cylinder is always less than that expected for a stationary cylinder at the same Reynolds number. Furthermore, there exist two ranges of flow velocities in which the wake frequency remains almost constant.

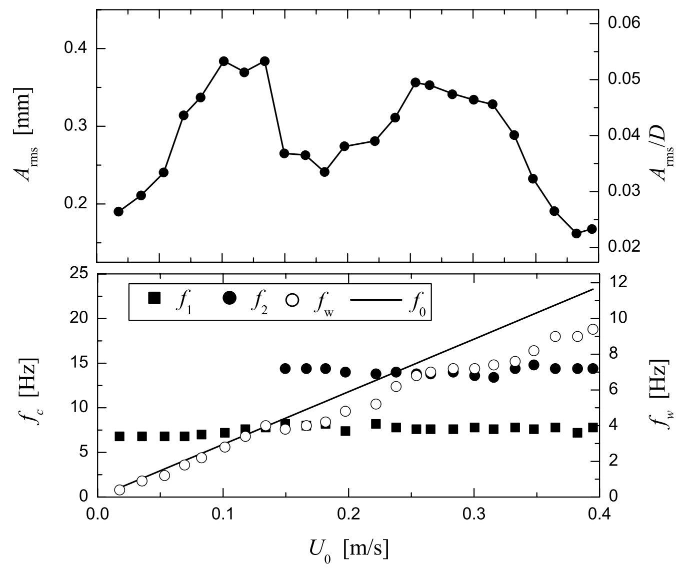

FIGURE 7. AMPLITUDE AND FREQUENCY RESPONSE OF THE VIBRATING CYLINDER FOR STEADY INCIDENT FLOW.

The present study deals with the effect of flow pulsations at a constant flow velocity of $U_0 = 0.30$ m/s corresponding to a Reynolds number of 2160, i.e. in the second response branch. Figure 8 shows a time record of the cylinder's tip displacement and its angular deflection for steady incident flow at the same Reynolds number. The angular deflection and the tip displacement follow the same oscillating pattern which indicates that the overall motion of the cylinder is dominated by the rotation of the cylinder about its supported end rather than by its translation. Both exhibit considerable amplitude modulations and involve biharmonic vibrations at frequencies $f_1 = 7.8$ Hz and $f_2 = 13.6$ Hz as can be verified by the power-spectral density of the displacement signal shown in Fig. 9. The coupling between the two frequency components is manifested by the existence of peaks at various combinations of the main peaks, $f_1 + nf_2$, where n is an integer number. The power spectra of the wake fluctuations in Fig. 10, display a predominant peak at 7.2 Hz, which is between f_1 and $\frac{1}{2}f_2$, and a less pronounced at the first

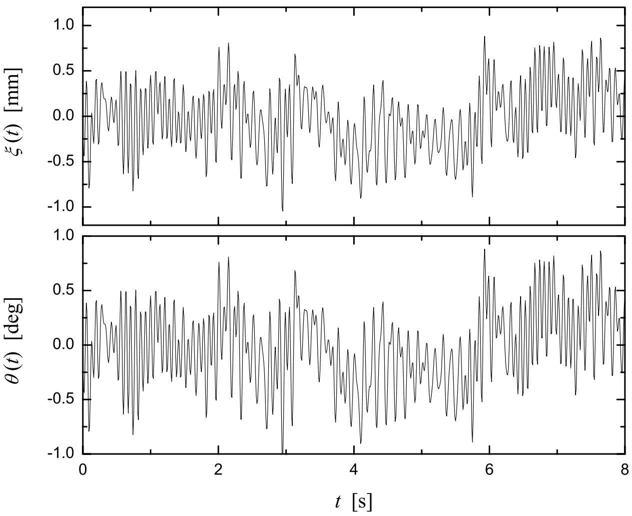

FIGURE 8. TIME-RESOLVED MEASUREMENTS OF THE TIP DISPLACEMENT AND THE ANGULAR DEFLECTION OF THE CYLINDER FOR STEADY INCIDENT FLOW AT $Re = 2160$.

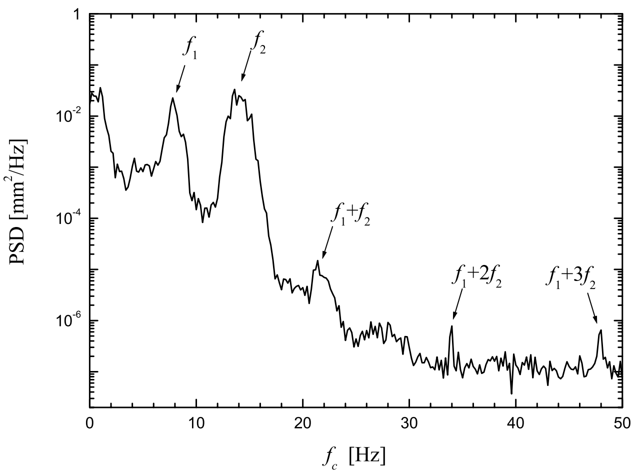

FIGURE 9. POWER-SPECTRAL DENSITY OF THE CYLINDER TIP DISPLACEMENT FOR STEADY FLOW AT $Re = 2160$.

superharmonic of the main wake frequency. It should be noted that a frequency of alternating vortex shedding f_w induces an excitation at $2f_w$ in the streamwise direction.

Pulsed Flow

Measurements were made for pulsation frequencies in the range f_e = 7.8–19.2 Hz at a constant pulsation amplitude of $\Delta U = 0.03$ m/s and constant mean velocity of $U_0 = 0.30$ m/s which corresponds to a Reynolds number of 2160. The amplitude and frequency response of the vibrating cylinder is shown in Fig. 11. The amplitude response displays two maxima at f_e = 11.1 and 15.0 Hz with peak values of 17% and 13% of the cylinder diameter, respectively. The peak values are approximately four times higher than the r.m.s. displacement induced by the flow pulsation $(= \Delta U / \sqrt{8}\pi f_e)$ which is shown by a dashed line on upper plot in Fig. 11. As the pulsation frequency increases above these points, the amplitude decreases almost linearly. This results in a trough at $f_e = 14.6$ Hz with a corresponding local minimum of $A_{\text{rms}} = 0.061D$. An overall minimum value of $0.048D$ in the r.m.s. amplitude is observed at the highest pulsation frequency which is comparable to $0.046D$ measured for steady incident flow at the same Reynolds number. However, the oscillation of the cylinder is much more regular in pulsed flow as shown in Fig. 12. This regularity might be attributed to the fact that the vibration frequency ‘locks on’ to the pulsation frequency (note that most of the full symbols are masked by the open symbols in the lower plot in Fig. 11).

Figures 13 and 14 show the power-spectra densities of the tip displacement signal for two representative pulsation frequencies. For each case, there is predominant peak at f_e whose power is substantially higher than the other peaks appearing at the superharmonics of f_e (cf. the difference in the scale of the vertical axis in Fig. 9 for steady flow). The peaks in the spectra are very clear and narrow band which further demonstrates the lock-on phenomenon. The displacement spectra were very similar for all pulsation frequencies tested and indicate that the vibration frequency can shift away from the natural frequencies of the structure. This behavior contrasts sharply the response observed in steady flow where the vibration frequencies remain almost unaltered by fluid forcing from the unsteady wake. It should also be pointed out that there were actually two co-existent

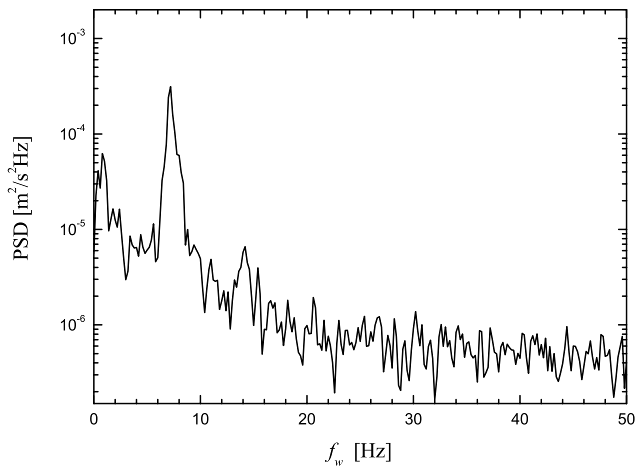

FIGURE 10. POWER-SPECTRAL DENSITY OF THE WAKE FLUCTUATIONS FOR STEADY FLOW AT $Re = 2160$.

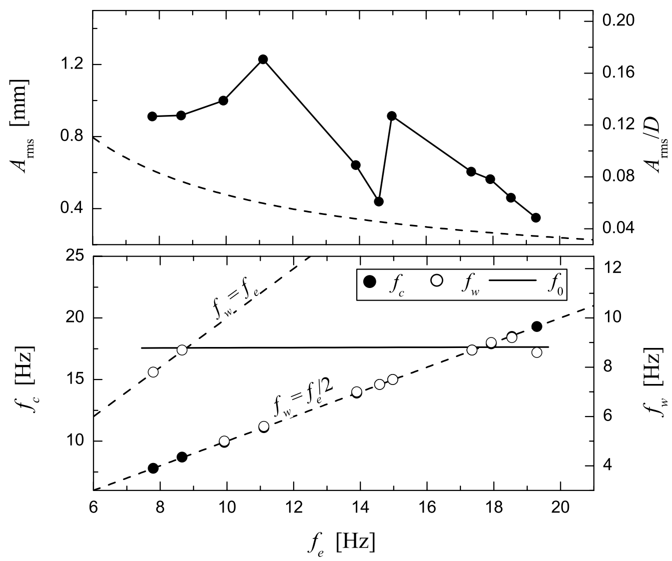

FIGURE 11. AMPLITUDE AND FREQUENCY RESPONSE OF THE VIBRATING CYLINDER FOR PULSED INCIDENT FLOW.

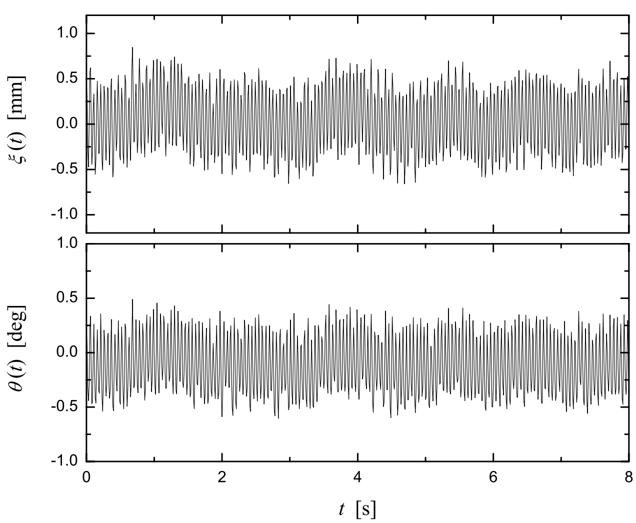

FIGURE 12. TIME-RESOLVED MEASUREMENTS OF THE TIP DISPLACEMENT AND THE ANGULAR DEFLECTION OF THE CYLINDER FOR PULSED INCIDENT FLOW AT $f_e = 19.3$ Hz.

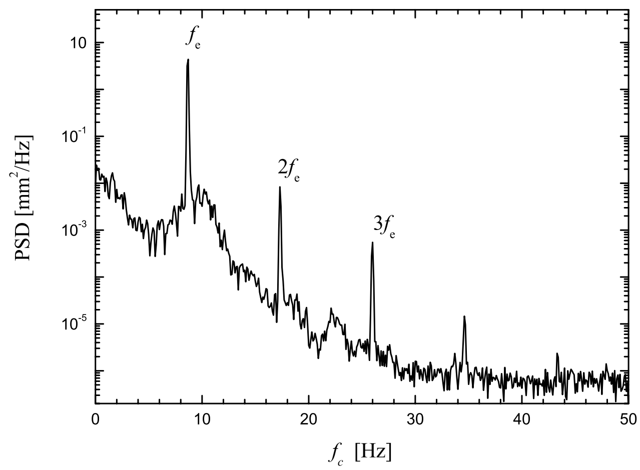

FIGURE 13. POWER-SPECTRAL DENSITY OF THE CYLINDER TIP DISPLACEMENT FOR PULSED FLOW AT $f_e = 8.7$ Hz.

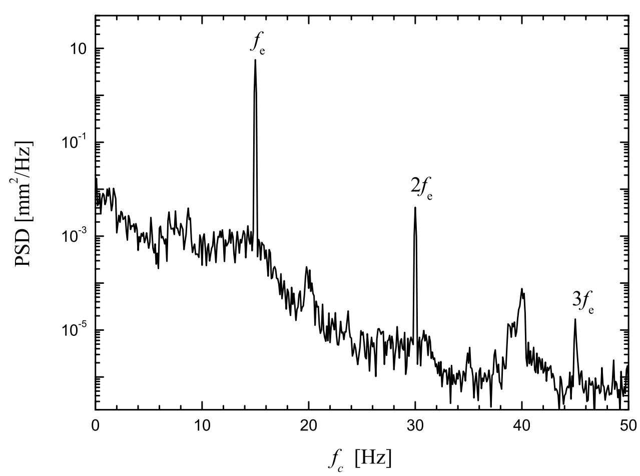

FIGURE 14. POWER-SPECTRAL DENSITY OF THE CYLINDER TIP DISPLACEMENT FOR PULSED FLOW AT $f_e = 15.0$ Hz.

frequencies f_1 and f_2 in the steady flow response corresponding to the main vibration modes of the structure.

The wake frequency provides very useful information in order to interpret the response of the vibrating cylinder. It can be observed in Fig. 11 that the predominant frequency in the wake locks on either to the pulsation frequency itself or its subharmonic as indicated by the dashed lines on the lower plot except for the highest pulsation frequency for which $f_w \approx f_0$. Figure 15 shows the power-spectral density of the wake fluctuations for a case where the main peak locks-on to the pulsation frequency, $f_e = 8.7$ Hz. A dominant narrow-band peak in the spectra occurs at f_e whereas another broad-band peak is observed around $\frac{1}{2} f_e$ which might indicate that the wake locks-on intermittently at half the pulsation frequency. Based on spectral characteristics obtained in the wake of a fixed cylinder in pulsating flow, it is suggested that a symmetric vortex shedding mode materializes at $f_e \approx f_0$ in this case (see Ref. [8] for an overview of the symmetric shedding mode). This hypothesis might account for

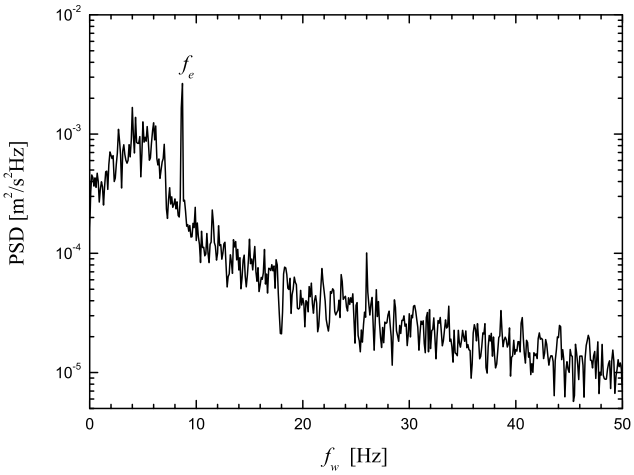

FIGURE 15. POWER-SPECTRAL DENSITY OF THE WAKE FLUCTUATIONS FOR PULSED FLOW AT $f_e = 8.7$ Hz.

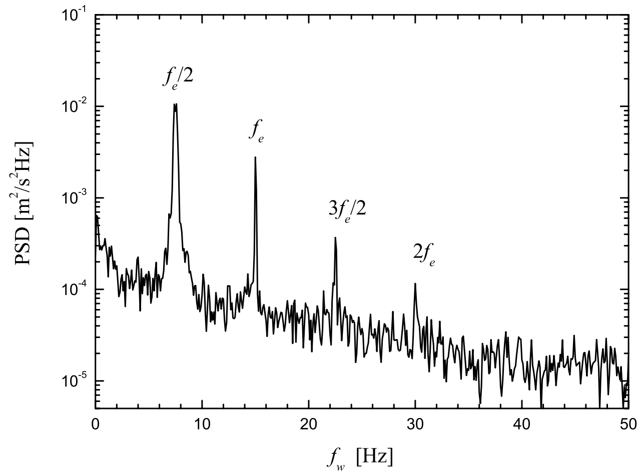

FIGURE 16. POWER-SPECTRAL DENSITY OF THE WAKE FLUCTUATIONS FOR PULSED FLOW AT $f_e = 15.0$ Hz.

the enhancement of the vibration amplitude at the pulsation frequency compared to that for steady incident flow (see Fig.13). As the pulsation frequency increases at constant mean velocity, the ratio f_e/f_0 also increases and the primary lock-on range which corresponds to alternating shedding, is approached. In this case, the vortex shedding frequency in the wake locks-on at half the pulsation frequency as demonstrated from the power-spectral density shown in Fig. 16. The spectra also contain peaks at the superharmonics of the shedding frequency which is consistent with the lock-on phenomenon [10]. The range of frequencies for which lock-on at $\frac{1}{2}f_e$ occurs corresponds to frequency ratios in the range $f_e/f_0 = 1.26$ to 2.09.

Figure 17 shows the variation in the relative power of the cylinder vibrations and the wake fluctuations as estimated by the magnitude of the corresponding spectral peaks. Although the magnitude of the peaks in the power-spectral densities do not represent power, strictly speaking, they provide an acceptable estimate of the relative power since all the peaks are sufficiently narrow-band. The striking observation in Fig. 17 is that the wake fluctuations are most enhanced when the vibration amplitude is relatively low, and vice versa. This paradoxical phenomenon is in-line with the findings of a previous related work by some of the authors on perturbed flow over a fixed cylinder [7]. There, it has been suggested that the excitation region of streamwise vibrations of elastically-supported cylinders does not coincide with the vortex lock-on region where the fluid forcing on the cylinder is magnified. The present results are more complicated due to the existence of two structural modes and their vibration shapes. However, the results clearly suggest that $f_e = 11.1$ Hz (i.e. $f_e/f_0 = 1.26$) falls within the lock-on region and the wake frequency locks on to half the pulsation frequency ($f_w = f_e/2 = 5.5$ Hz) which is consistent with the lock-on map in the amplitude–frequency plane [10]. Furthermore, it has been found that the phase of the fluid-induced forces with respect to the cylinder vibration becomes more positive as the frequency ratio f_e/f_0 reduces below a critical value of 2.0 [6, 18, 19]. Therefore, it is plausible that the vibration response is maximized under these pulsed flow conditions which result in lock-on for the lowest value of the ratio f_e/f_0.

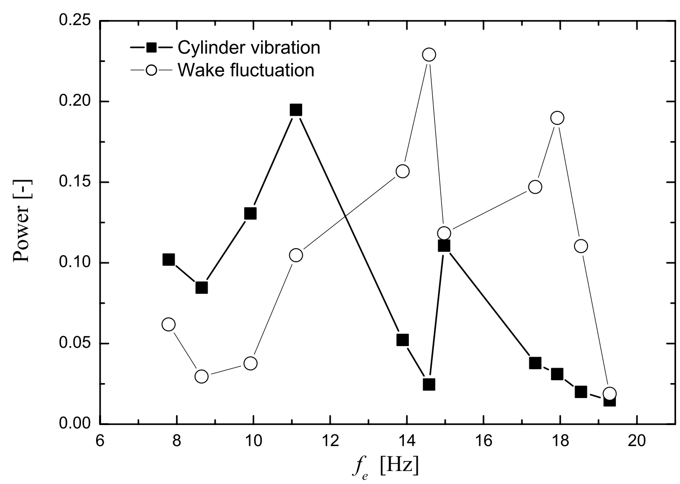

FIGURE 17. RELATIVE POWER IN THE CYLINDER VIBRATIONS AND THE WAKE FLUCTUATIONS.

CONCLUSIONS

The main conclusions drawn from the present study are the following:

1. A cantilevered cylinder with two degrees-of-freedom to translate and rotate in the streamwise direction exhibits two excitation branches in steady incident flow associated with two different vibration mode shapes. Single-harmonic vibrations at the natural frequency of the first mode occur in the first branch whereas biharmonic vibrations involving both natural frequencies were found in the second branch.
2. Extraneously-imposed flow pulsations can take over control of both the cylinder and the wake response. For all pulsation frequencies employed in the present experiments, the cylinder vibrations locked-on to the excitation frequency but the wake fluctuations exhibited a more complex response.
3. The amplitude of the pulsation-induced vibrations is much higher than the amplitude of the imposed pulsations.
4. The structure and the wake have their own natural frequencies and flow-induced vibration results from their interaction. The frequencies at which the structure can absorb most of the energy from the wake do not correspond to those at which the fluid forcing from the unsteady wake is most enhanced.

The present results may be useful to better understand the differences between the 'vortex lock-on' observed in the response of cylinder wakes to forced excitation and the 'lock-in vibration' observed in the response of elastically-supported cylinders to self-excitation from the wake.

ACKNOWLEDGMENT

The authors would like to thank Jonathan Dusting for his help with the development of the imaging technique.

REFERENCES

[1] Bearman, P. W., 1984. "Vortex shedding from oscillating bluff bodies". *Ann. Rev. Fluid Mech.*, ***16***, pp. 195–222.

[2] Naudascher, E., 1987. "Flow-induced streamwise vibrations of structures". *J. Fluids Struct.*, ***1***, pp. 265–298.

[3] Sarpkaya, T., 2004. "A critical review of the intrinsic nature nature of vortex-induced vibrations". *J. Fluids Struct.*, ***19***, pp. 389–447.

[4] King, R., 1977. "A review of vortex shedding research and its application". *Ocean Eng.*, ***4***, pp. 141–171.

[5] Okajima, A., Kosugi, T., and Nakamura, A., 2002. "Flow-induced in-line oscillation of a circular cylinder in a water tunnel". *Trans. ASME: J. Press. Vessel Tech.*, ***124***, pp. 89–96.

[6] Nishihara, T., Kaneko, S., and Watanabe, T., 2005. "Characteristics of fluid dynamic forces acting on a circular cylinder oscillated in the streamwise direction and its wake patterns". *J. Fluids Struct.*, ***20***, pp. 505–518.

[7] Konstantinidis, E., Balabani, S., and Yianneskis, M., 2005. "The timing of vortex shedding in a cylinder wake imposed by periodic inflow perturbations". *J. Fluid Mech.*, ***543***, pp. 45–55.

[8] Konstantinidis, E., and Balabani, S., 2007. "Symmetric vortex shedding in the near wake of a circular cylinder due to streamwise perturbations". *J. Fluids Struct.*, ***23***, pp. 1047–1063.

[9] Griffin, O. M., and Hall, M. S., 1991. "Vortex shedding lock-on and flow control in bluff body wakes – Review". *Trans. ASME: J. Fluids Eng.*, ***113***(4), pp. 526–537.

[10] Konstantinidis, E., Balabani, S., and Yianneskis, M., 2003. "The effect of flow perturbations on the near wake characteristics of a circular cylinder". *J. Fluids Struct.*, ***18***, pp. 367–386.

[11] Konstantinidis, E., Balabani, S., and Yianneskis, M., 2005. "Conditional averaging of PIV plane wake data using a cross-correlation approach". *Exp. Fluids*, ***39***, pp. 38–47.

[12] Konstantinidis, E., and Balabani, S., 2008. "Flow structure in the locked-on wake of a circular cylinder in pulsating flow: Effect of forcing amplitude". *Int. J. Heat Fluid Flow*, ***29***(6), pp. 1567–1576.

[13] Peeran, S. Y., 2007. "Design of a test apparatus for free cylinder oscillation experiments". Master's thesis, Department of Mechanical Engineering, King's College London.

[14] Blevins, R. D., 2001. *Flow-induced vibration*. Krieger Publishing Company, Florida.

[15] Zhang, H. J., Zhou, Y., So, R. M. C., Mignolet, M. P., and Wang, Z. J., 2003. "A note on the fluid damping of an elastic cylinder in a cross-flow". *J. Fluids Struct.*, ***17***, pp. 479–483.

[16] Akaike, H., 1974. "A new look at the statistical model identification". *IEEE Trans. Automatic Control*, ***19***(6), pp. 716–723.

[17] Zdravkovich, M. M., 1997. *Flow around circular cylinders*, Vol. 1. Oxford University Press.

[18] Balabani, S., Konstantinidis, E., Liang, C., and Papadakis, G., 2007. "Numerical study of the effect of velocity perturbations on the mechanics of vortex shedding in synchronized bluff-body wakes". In 5th Conf. on Bluff Body Wakes and Vortex-Induced Vibrations - BBVIV5, Leweke, T., Meneghini, J. R. and Williamson, C. H. K., ed., Costa do Sauípe, Bahia, Brazil, pp. 241–244.

[19] Liang, C., and Konstantinidis, E., 2008. "Determination of fluid forces on a circular cylinder in pulsating cross-flow from numerical experiments". In Proc. of the 9th Int. Conf. on Flow-Induced Vibration - FIV2008, Zolotarev, I. and Horàček, J., ed., Prague, Czech Republic, pp. 91–96.